3D NEUROLOGICAL IMAGE RETRIEVAL WITH LOCALIZED PATHOLOGY-CENTRIC CMRGLC PATTERNS

Weidong Cai[1], *Sidong Liu*[1], *Lingfeng Wen*[1,2], *Stefan Eberl*[1,2], *Michael J Fulham*[1,2,3], *Dagan Feng*[1,4]

[1] Biomedical and Multimedia Information Technology (BMIT) Research Group, School of Information Technologies, University of Sydney, Australia
[2] Department of PET and Nuclear Medicine, Royal Prince Alfred Hospital, Sydney, Australia
[3] Sydney Medical School, University of Sydney, Australia
[4] Centre for Multimedia Signal Processing (CMSP), Department of Electronic & Information Engineering, Hong Kong Polytechnic University, Hong Kong

ABSTRACT

Functional neuroimaging has an important role in non-invasive diagnosis of neurodegenerative disorders. There are now large volumes of imaging data generated by functional imaging technologies and so there is a need to efficiently manage and retrieve these data. In this paper, we propose a new scheme for efficient 3D content-based neurological image retrieval. 3D pathology-centric masks were adaptively designed and applied for extracting CMRGlc (cerebral metabolic rate of glucose consumption) texture features with volumetric co-occurrence matrices from neurological FDG PET images. Our results, using 93 clinical dementia studies, show that our approach offers a robust and efficient retrieval mechanism for relevant clinical cases and provides advantages in image data analysis and management.

Index Terms— 3D neurological image, image retrieval, brain PET image, dementia, localized retrieval

1. INTRODUCTION

Functional neuroimaging technologies, such as positron emission tomography (PET), play an important role in understanding neurobiology and in clinical diagnosis. Functional neuroimaging can detect abnormalities before there are changes on anatomical imaging; it also has a role in the assessment of therapy and monitoring disease progression. Instrumentation advances in neuroimaging devices have resulted in large volumes of imaging data and the need for larger image archives and repositories. Further, with the greater volume of imaging data more effective approaches for image retrieval and management are required. Retrieval of neurological images based on image-related features could provide an alternative or complement the traditional approach of text based searches and retrieval based on patient demographic data. Clinicians could then more efficiently retrieve relevant clinical cases [1, 2, 3].

Various content-based neurological image retrieval systems have been reported. We previously proposed a dynamic brain PET image retrieval system based on physiological kinetic features associated with pixel-wise tissue time activity curve (TTAC) clustering [4]. Wong *et al*. [5] established a neuro-informatics database system (NIDS) with co-registered static PET and MR image data for temporal lobe epilepsy studies, supporting image retrieval based on geometric location, metabolic counts of glucose consumption and textual features from the file header of images. We also extended our earlier work with a volume of interest (VOI)-based retrieval system for dynamic 3D brain PET images with VOI-segmented images using a fuzzy C-means cluster analysis and region-growing approach [6]. VOI functional TTACs, Zubal-phantom-labeled VOI locations, and textual attributes (from the image file header) were used for region-based volumetric image retrieval. Most recently, Batty *et al*. [7] designed a PET image retrieval system based on the Talairarch and Tournoux atlas [8] to define distinct regions of interest (ROI). They extracted a combined ROI feature set consisting of anatomical texture patterns using 2D Gabor filters [9] and a related mean index ratio with PET activity measurements in the image retrieval of dementia cases.

These systems were mainly based on physiological functional features with reconstructed raw PET activity (normal uptake) values [5] and related mean activity levels [7], or dynamic TTAC vectors [4, 6]. Raw PET activity relying on static imaging protocols may give rise to unreliable content-based neurological image retrieval systems as the raw PET activity values are affected by several factors, such as the uptake time, injected dose and patient to patient variations. Dynamic imaging protocols, meanwhile, require substantially longer imaging times, which are not practical in a clinical environment. The cerebral metabolic rate of glucose consumption (CMRGlc) is an absolute quantitative functional parameter, which can be derived by static [^{18}F] *2-fluoro-deoxy-glucose* (FDG) brain PET imaging as long as a plasma activity concentration input function can be obtained. CMRGlc depicts cerebral glucose consumption and can facilitate the detection of abnormalities. We propose a new neurological image CBIR approach based on localized pathology-centric CMRGlc patterns using a new adaptive knowledge-based approach and 3D pathology-centric masks (PCMs). We tested our approach on 93 clinical neurological FDG-PET studies.

2. METHODS

2.1. Volumetric Image Pre-processing

2.1.1. Generation of Physiological CMRGlc Images

The autoradiographic (ARG) approach [10] was used to derive the CMRGlc images from raw static 3D PET image data (see Fig.1 (a)):

$$CMRGlc_i = C_{glu} \times \frac{\left\{ C_i(T) - \frac{k_1}{\alpha_2 - \alpha_1}\left[(k_4 - \alpha_1)e^{-\alpha_1 t} + (\alpha_2 - k_4)e^{-\alpha_2 t}\right] \otimes C_p(t) \right\}}{(LC)\frac{k_2 + k_3}{\alpha_2 - \alpha_1}(e^{-\alpha_1 t} - e^{-\alpha_2 t}) \otimes C_p(t)} \quad (1)$$

where C_{glu} is the endogenous glucose concentration in plasma, LC denotes the lumped constant, $t = 1, 2, \ldots, T$ are discrete sampling times of the measurements, $C_i(T)$ is the measured tissue activity at time T for the ith voxel, $C_p(t)$ represents plasma time activity curve, $k_1 \sim k_4$ are the population mean rate constants for the grey matter in human brain, and

$$\alpha_{1,2} = \frac{1}{2}\left\{(k_2 + k_3 + k_4) \mp \sqrt{(k_2 + k_3 + k_4)^2 - 4k_2k_4}\right\} \quad (2)$$

2.1.2. Spatial Normalization

To facilitate content-based retrieval, the generated CMRGlc parametric image volume with dimensions of 128×128×56 and a voxel size of 1.840×1.840×3.375 mm^3 were spatially normalized to a PET brain template using the SPM2 package (Wellcome Trust Centre for Neuorimaging, London, U.K.) [11]. The transformed standardized brain volume has dimensions of 91×109×91 voxels with a voxel size of 2×2×2 mm^3. The MNI-based Tzourio-Mazoyer atlas [12] was then used to define 116 Volumes of Interest (VOI), including 90 regions for both hemispheres, 18 regions for cerebellum and 8 regions for the cerebellar vermis.

2.2. Construction of Pathology-Centric Masks (PCMs)

2.2.1. Knowledge-based Initial PCM Design

Different types of dementia affect different brain regions so it is unlikely that a single general mask could be adopted to label all the disorders. So we constructed a set of pathology-centric masks based on domain knowledge extracted from the clinical neuroimaging literature and expert clinical guidance [13, 14]. The PCM of Alzheimer's disease (AD) shown in Fig.1 (f) upper row, consisted of 37 Tzourio-Mazoyer defined regions and there were 27 regions for the PCM of fronto-temporal dementia (FTD) shown in Fig.1 (f) lower row.

2.2.2. Adaptive PCM Refinement with T-map

To further utilize the intrinsic information contained in the CMRGlc images, the PCMs were adaptively refined based on the T-map (voxel by voxel t-test on all voxels), given as following:

$$\text{T-map}_i = \frac{CMRGlc_i - Mean_i}{SD_i} \quad (3)$$

where $Mean_i$ and SD_i stand for the mean and standard deviation of all the ith voxels from spatially normalized CMRGlc images of 15 normal cases. Assuming that the CMRGlc values for a given voxel are normally distributed, then values which fall outside a defined interval can be assumed to be abnormal. We defined the threshold for abnormality as the lower limit of the 95% confidence interval because dementias exhibit hypo-metabolic patterns. For every case diagnosed with same disorder, its T-map captured the voxel-based abnormal regions (see Fig.1 (e)), which were consequently added to the initial PCM corresponding to that disorder (see Fig.1 (g)). Finally, all the PCMs were refined by accumulating those affected regions.

2.3. Feature Extraction

2.3.1. Functional Normalization of CMRGlc Images

Although the CMRGlc images, derived by Eq. (1), were spatially normalized, there may still be a bias due to the overall activity scale disparities between different PET scans. Therefore, the images were further normalized to drive the FN_CMRGlc images defined as the CMRGlc values divided by the mean of cerebellum region (for FTD see Fig. 1 (c) upper row) or whole cortex (for other disorders see Fig. 1 (c) lower row). Such functional normalization of CMRGlc could be used to enhance the magnitude of the hypo-metabolic differences between different types of dementia thus increasing the discriminative power of the CMRGlc patterns.

2.3.2. PCM-based Volumetric Texture Feature Extraction

Texture is one of the most commonly used visual features in CBIR for neurological images, and can be extracted by Gabor filters or co-occurrence matrices techniques [15]. Gabor filters are powerful edge/line/bar detectors and have orientation and frequency tunable properties. However, they are used under the assumption that the texture patterns are homogenous, which is not always the case, especially in functional images. The co-occurrence matrices approach, on the other hand, allows for capturing the spatial dependence of grey-levels, which contributes to the perception of texture, and also detects some abnormalities in images that are beyond human visual perception [16]. This technique constructs co-occurrence matrices based on different orientations and distance between image pixels and extracts meaningful statistics from the matrices as texture representations. In the approach using 2D co-occurrence matrices, given a distance d at an orientation angle θ, $p_{(d,\theta)}(l_1, l_2)$, the (l_1, l_2) coefficient of the corresponding matrix $\mathbf{P}_{(d,\theta)}$, is the co-occurrence count or probability of going from a grey level l_1 to another grey level l_2 with an inter-sample spacing of d along the axis making an angle θ with the x axis. The information in the matrices can then be further extracted by deriving a set of second-order statistical quantities, called Haralick feature descriptors. A preliminary study [17] showed that 3D textures derived from volumetric data are likely to have better discriminative power than 2D textures derived from separated slice data. Therefore, we developed a three-step PCM-based volumetric texture feature extraction approach with co-occurrence matrices as follows:

Step-1*: PCM-based volume extraction* – For a given 3D parametric image, PCMs are applied to filter out the irrelevant regions. The parametric image is then reshaped to a smaller volume which contains only the VOI related to the associated disorder;

Step-2*: 3D co-occurrence matrix transformation* – The results from step-1 are further transformed into 3D co-occurrence matrices. Nine slices are obtained to represent the reshaped volume. These slices account for different planes across the volume corresponding to the 13 directions set by two orientation angles θ and φ, where θ indicates the angle in horizontal plane (same as in 2D co-occurrence matrices approach), and φ means the angle in vertical plane.

Step-3*: Volumetric texture feature quantification* – Eleven Haralick feature descriptors are implemented: *Energy*, *Entropy*, *Contrast*, *Variance*, *Correlation*, *Difference Entropy*, *Difference Variance*, *Inverse Difference Moment*, *Sum Entropy*, *Sum Variance* and *Sum Average*. These features are extracted from all nine slices and further fused to give the representation of the whole volume.

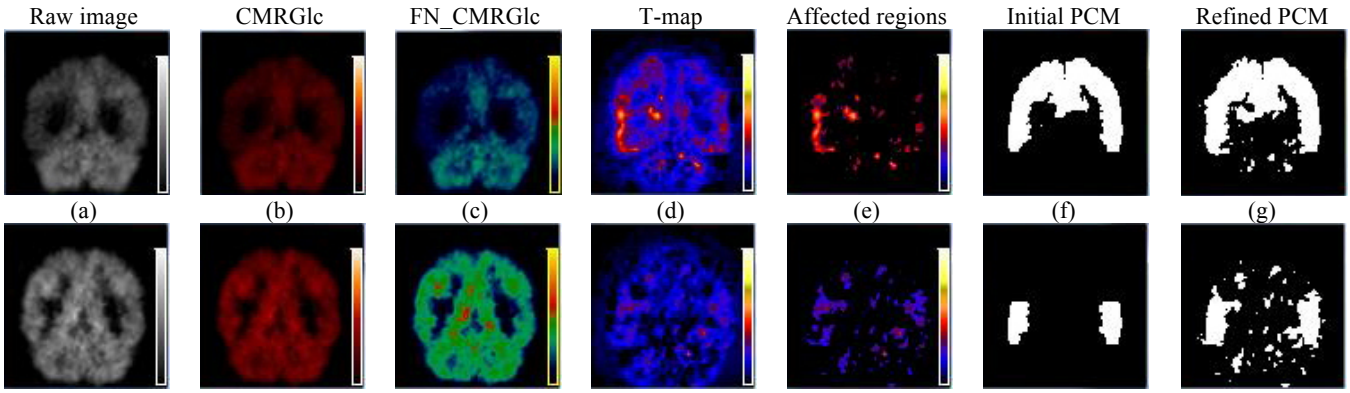

Fig.1 Coronal views (91×91 at the 33rd plane) of: (a) raw 3D FDG PET image; (b) parametric image of CMRGlc; (c) functional normalized CMRGlc image; (d) T-map; (e) affected regions associated with T-map; (f) initial PCM; (g) refined PCM with T-map from Patient #2431 with AD (upper row) and Patient #7274 with a FTD (lower row), spatially normalized by SPM2.

2.4. Similarity Measurement and Performance Evaluation

2.4.1. Similarity Measurement

Before the similarity measurement, the derived feature vectors were further normalized. The top 5% of the distribution within each feature space was eliminated since these extreme values are most likely due to noise. In addition, all the values within the feature space were divided by the nominal maximum of the remaining 95% of elements. The Euclidean distance was then used to measure the distance since the vectors were normalized to the same scale and the bias of extreme feature elements had already been eliminated. The distance was calculated sequentially between the query image and every image case in the database. After all the distances were obtained, the system ranked them automatically in ascending order.

2.4.2. Performance Evaluation

For this study, we used the conclusion from the imaging study and the diagnosis from the patients' reports. However, in some cases of dementia there can be a degree of overlap from one disorder to another because similar brain regions are affected and thus a definitive clinical or imaging diagnosis could not be made. These cases were classified as 'indefinite' and were mainly cases where the question was of AD or Diffuse Lewy Body disease (DLBD). To balance the impact caused by common regions shared by different disorders and to objectively describe the retrieval results, the following relevance criteria were considered: If the retrieval image belongs to the class of the query image, then the relevance score / weight factor was set to 1.0. For indefinite disorders, if the retrieval image belonged to either class which the query images related to, then the score was 0.75. If the retrieval result belonged to any abnormal class other than the classes it belonged to or related to, the score became 0.25. If the retrieved image did not belong to any abnormal class, the score was then set to 0. The retrieval performances were evaluated by a precision measurement, which was defined as the fraction of relevant images that are relevant to the query, i.e., the number of relevant items retrieved divided by number of items retrieved. The top ten retrieval results were counted for each query.

3. RESULTS

To validate the proposed retrieval approach, we set up a database of 93 clinical 3D neurological FDG-PET images that included patients with AD (n=16), FTD (n=16), indefinite disorders AD/DLBD (n=12), 34 other disorders of dementia and 15 normal cases. The studies were acquired on a CTI ECAT 951R whole body PET scanner, at the Department of PET and Nuclear Medicine, Royal Prince Alfred Hospital. Arterialized-venous blood samples were taken at 10 min and 45 min post injection to calibrate a population-based input function [18]. PET scanning commenced at least 30 min after tracer injection with a scan duration of twenty minutes.

Fig. 1 shows the results for cases of AD and a FTD. Our proposed localized PCM-based retrieval approach with FN_CMRGlc texture feature (LR_FN_CMRGlc) was compared with three other retrieval methods: (1) a localized PCM-based retrieval method with CMRGlc (without functional normalization) texture feature (LR_CMRGlc); (2) a global (without PCM) retrieval method with FN_CMRGlc texture feature (GR_FN_CMRGlc); and (3) a global retrieval method with CMRGlc texture feature (GR_CMRGlc). For each retrieval method, a *leave-one-out* test was conducted with a total 44 queries,

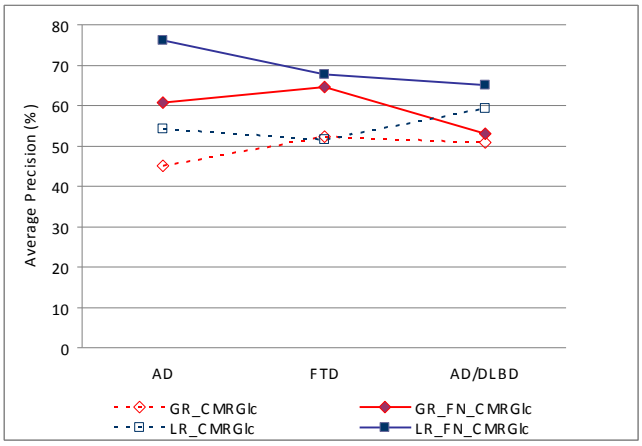

Fig.2 Performance comparison of four different retrieval methods

including 16 AD, 16 FTD and 12 AD/DLBD cases, while for each disorder group, every case image was used as the query image and overall performance was the average precision of all the queries. The comparison results are shown in Fig. 2, and demonstrate that our LR_FN_CMRGlc method had the best performance, for single cases and also indefinite disorders. The results also indicated that (1) the localized PCM-based method had better performance than the global methods, particularly for AD cases (12% higher) and AD/DLBD cases (10% higher); and (2) the retrieval methods with functional normalized CMRGlc texture feature had better performance than the methods with CMRGlc texture feature, particularly for AD cases (19% higher) and FTD cases (14% higher). In addition, to validate the functional normalization of CMRGlc images for FTD cases, we conducted a comparison study, which showed that the normalization with the mean of cerebellum was better than the mean of whole cortex, for both localized retrieval method (13% higher) and the global method (9% higher).

4. CONCLUSION

We present a localized 3D neurological image retrieval technique based on pathology-centric CMRGlc texture patterns. Our results show that our method was efficient in retrieving relevant image cases and could facilitate the statistical and comparative analysis of functional neurological image data.

5. ACKNOWLEDGEMENT

This work was supported in part by ARC and PolyU grants.

6. REFERENCES

[1] H. Muller, N. Michoux, D. Bandon, and A. Geissbuhler , "A review of content-based image retrieval systems in medical applications – clinical benefits and future directions," *International Journal of Medical Informatics*, vol. 73, pp.1-23, 2004.

[2] W. Cai, J. Kim and D. Feng, "Chapter 4 – Content-based Medical Image Retrieval", in *Biomedical Information Technology*, pp83-113, Edited by D. Feng, Elsevier, San Diego, USA, 2008.

[3] L.R. Long, S. Antani, T.M. Deserno and G.R. Thoma, "Content-based Image Retrieval in Medicine: Retrospective Assessment, State of the Art, and Future Directions", *International Journal of Healthcare Information Systems and Informatics*, vol. 4, no. 1, pp.1-16, 2009.

[4] W. Cai, D. Feng and R. Fulton, "Content-Based Retrieval of Dynamic PET Functional Images", *IEEE Transactions on Information Technology in Biomedicine*, vol. 4, no. 2, pp.152-158, 2000.

[5] S.T.C. Wong, K.S. Hoo, X. Cao, D. Tjandra, J.C. Fu, and W.P. Dillon, "A neuroinformatics database system for disease-oriented neuroimaging research", *Academic Radiology*, vol. 11, no. 3, pp.345-358, 2004.

[6] J. Kim, W. Cai, D. Feng, and H. Wu, "A new way for multi-dimensional medical data management: volume of interest (VOI)-based retrieval of medical images with visual and functional features", *IEEE Transactions on Information Technology in Biomedicine*, vol. 10, no. 3, pp.598-607, 2006.

[7] S. Batty, J. Clark, T. Fryer, and X. Gao, "Prototype system for semantic retrieval of neurological PET images", *The International Conference on Medical Imaging and Informatics (MIMI 2007), Aug 14-16, 2007, Beijing*, LNCS 4987, pp.179-188, 2008.

[8] J. Talairarch, P. Tournoux, "Co-planar stereotaxic atlas of the human brain", *Clinical Neurology and Neurosurgery*, vol. 91, no. 3, pp.277-278, 1989.

[9] B. S. Manjunath, W. Y. Ma, "Texture features for browsing and retrieval of image data", *IEEE Transactions on Pattern Analysis and Machine Intelligence*, vol. 18, no. 8, pp.837-842, Aug. 1996.

[10] G.D. Hutchins, J.E. Holden, R.A. Koeppe, *et. al.*, "Alternative approach to single-scan estimation of cerebral glucose metabolic rate using glucose analogs with particular application to ischemia", *Journal of Cerebral Blood Flow and Metabolism*, vol. 4, pp.35-40, 1984.

[11] R. Frackowiak, K.J. Friston, C.D. Frith, *et al.*, *Human Brain Function*. Amsterdam; Boston: Elsevier Academic Press, 2004.

[12] N. Tzourio-Mazoyer, B. Landeau, D. Papathanassiou, *et al.*, "Automated Anatomical Labeling of Activations in SPM Using a Macroscopic Anatomical Parcellation of the MNI MRI Single-Subject Brain," *NeuroImage,* vol. 15, no. 1, pp. 273-289, 2002.

[13] M. Brand, and H. Markowitsch, "Brain structures involved in Dementia," *Competence Assessment in Dementia*, pp.25-34, 2008.

[14] B. Ibach, S. Poljansky, J. Marienhagen, *et al.*, "Contrasting metabolic impairment in frontotemporal degeneration and early onset Alzheimer's disease," *NeuroImage,* vol. 23, no. 2, pp.4., 2004.

[15] R. M. Haralick, K. Shanmugam, I. Dinstein, "Texture features for image classification", *IEEE Trans. Sys., Man., and Cyb.*, vol.SMC-3, no. 6, 1973.

[16] D.S. Raicu, J.D. Furst, D. Channin, D. Xu, A. Kurani, and S. Aioanei, "A texture dictionary for human organs tissues'classification", *Proc. 8th SCI 2004*, USA, July 18-21, 2004.

[17] A.S. Kurani, D.H. Xu, J. Furst, and D.S. Raicu, "Co-occurrence matrices for volumetric data", *Proceedings of the 7th International Conference on Computer Graphics and Imagine (CGIM)*, Hawaii, 2004.

[18] S. Eberl, A.R. Anayat, R. Fulton, P.K. Hooper, and M.J. Fulham, "Evaluation of two population-based input functions for quantitative neurological FDG PET studies", *European Journal of Nuclear Medicine*, vol. 24, no. 3, pp.299-304, 1997.